

PRENER, J. S. (1967). *J. Electrochem. Soc.* **114**, 77–83.SICHER, H. (1962). *Oral Histology and Embryology*. St Louis: Mosby.STADELMANN, P. A. (1987). *Ultramicroscopy*, **21**, 131–146.

VOEGEL, J.-C. (1978). PhD thesis, Univ. Louis Pasteur, Strasbourg, France.

Acta Cryst. (1993). **B49**, 62–66

Structural Parameters and Electron Difference Density in Y_2BaCuO_5

BY R. H. BUTTNER AND E. N. MASLEN

Physics Department, University of Western Australia, Nedlands, WA 6009, Australia

(Received 5 February 1992; accepted 21 July 1992)

Abstract

Dyttrium barium copper(II) pentoxide, Y_2BaCuO_5 , $M_r = 458.7$, orthorhombic, $Pnma$, $a = 12.188$ (2), $b = 5.662$ (2), $c = 7.132$ (2) Å, $V = 492.17$ (3) Å³, $Z = 4$, $D_x = 6.19$ Mg m⁻³, $\lambda(\text{Mo } K\alpha) = 0.71069$ Å, $\mu = 36.633$ mm⁻¹, $F(000) = 812$, $T = 298$ K, final $R = 0.059$, $wR = 0.028$ for 2758 unique reflections. The structural parameters for the nonsuperconducting 'green phase' Y_2BaCuO_5 were redetermined and the electron density compared with that for the high- T_c superconductor $YBa_2Cu_3O_{7-\delta}$. The $\Delta\rho$ topography near Cu in Y_2BaCuO_5 resembles that near Cu2 in $YBa_2Cu_3O_{7-\delta}$, which has similar coordination. It differs markedly from that near Cu1, which coordinates with disordered O atoms. The similarity of both coordination and electron density for the Cu atom in the green phase with those for Cu2 in the high- T_c compound is consistent with both atoms being in the +2 oxidation state.

Introduction

A nonsuperconducting green phase with the composition Y_2BaCuO_5 was first identified as a contaminant in the high-temperature superconductor $YBa_2Cu_3O_{7-\delta}$. A powder investigation by Michel & Raveau (1982) tentatively established the space group of Y_2BaCuO_5 to be $Pbnm$, which was confirmed in single-crystal studies by Watkins, Fronczek, Wheelock, Goodrich, Hamilton & Johnson (1988) and by Sato & Nakada (1989). The atomic positions for the two earlier studies were concordant, but the Y1 and Y2 vibration amplitudes from the first are markedly smaller than those from the second. Because Y_2BaCuO_5 is not affected by nonstoichiometry or disorder, its structural geometry and $\Delta\rho$ topography can be usefully compared with those of the Cu atoms in the high- T_c compound. A further objective for a more accurate study is to check the vibration amplitudes.

Table 1. *Experimental and refinement data for Y_2BaCuO_5*

Scan type	$\omega/2\theta$
Scan speed	6.51° min ⁻¹
Peak scan width ($a + b \tan\theta$)	1.64; 0.71°
Maximum 2θ	100°
Maximum variation in intensity of standards $\pm 600 \pm 040 \pm 004$	1.3%
Number of reflections measured	22779
Transmission range in absorption corrections	0.23; 0.36
R_{int} (before and after absorption)	0.086; 0.071
Number of independent reflections $0 \leq h \leq 26$, $0 \leq k \leq 12$, $0 \leq l \leq 15$	2758
R	0.059
wR	0.028
S	1.66 (2)
Maximum height in final difference Fourier map	7.6 (9) e Å ⁻³
Minimum height in final difference Fourier map	-6.6 (9) e Å ⁻³
Minimum extinction y	0.67

With the assumption of the normal oxidation states of +2 for Ba, +3 for Y and -2 for O, charge balance requires that Cu for Y_2BaCuO_5 be in the +2 state. Nevertheless, its fivefold coordination closely resembles that of Cu2 in $YBa_2Cu_3O_{7-\delta}$, frequently cited as having an oxidation number that approaches +3 as δ decreases from 0.5. Some theoretical treatments relate the superconductivity of the high- T_c material to the Cu2-atom oxidation number. In that context the electron density near the Cu atom in the stoichiometric compound Y_2BaCuO_5 provides a reference standard.

Buttner & Maslen (1992) have recently shown that $\Delta\rho$ maps for the high-temperature superconductor $YBa_2Cu_3O_{7-\delta}$ are related to the structural geometry. The $\Delta\rho$ topography near the Cu1 atom adjacent to the O-atom defects is similar to that near atoms with elongated octahedral coordination in well defined +2 states such as Cu in $KCuF_3$ (Buttner, Maslen & Spadaccini, 1990). On the other hand, the electron density near Cu2, which has fivefold coordination and is not affected directly by oxygen disorder, has

Table 2. *Positional and anisotropic thermal parameters* ($\text{\AA}^2 \times 10^4$) *for* Y_2BaCuO_5

$$T = \exp[-2\pi^2(a^*h^2U_{11} + b^*k^2U_{22} + c^*l^2U_{33} + 2a^*b^*hkU_{12} + 2a^*c^*hlU_{13} + 2b^*c^*lkU_{23})].$$

	x	y	z	U_{11}	U_{22}	U_{33}	U_{12}	U_{13}	U_{23}
Y1	0.07386 (3)	0.75	0.39582 (6)	36 (1)	43 (2)	39 (2)	0.0	1 (1)	0.0
Y2	0.28826 (3)	0.75	0.11627 (6)	32 (1)	45 (2)	45 (2)	0.0	1 (1)	0.0
Ba	0.09518 (2)	0.25	0.06986 (4)	56 (1)	65 (1)	89 (1)	0.0	-9 (1)	0.0
Cu	0.65934 (4)	0.75	0.71265 (8)	43 (2)	48 (2)	55 (2)	0.0	11 (2)	0.0
O1	0.5676 (2)	0.5069 (5)	0.8349 (3)	56 (7)	62 (9)	79 (9)	-7 (7)	0 (7)	8 (7)
O2	0.7720 (2)	0.5038 (5)	0.6439 (3)	70 (8)	69 (10)	96 (10)	33 (7)	13 (7)	18 (8)
O3	0.6004 (3)	0.75	0.4206 (5)	40 (10)	120 (14)	78 (13)	0.0	13 (10)	0.0

no strong features. That is also true near Y and Ba, where the $\Delta\rho$ topography does not correlate strongly with structural geometry as defined by the coordinating O atoms. There were mild differences between $\Delta\rho$ topographies near Y, Ba and Cu2 for samples with different values of δ .

Experimental

After preliminary heating, powdered BaCO_3 , CuO and Y_2O_3 , mixed in the stoichiometric proportions for $\text{YBa}_2\text{Cu}_3\text{O}_7$, were heated to a peak temperature of 1343 K on a Ta_2O_5 plate. The Ta_2O_5 selectively absorbs a Cu-rich component from the melt. The residue consisted of prismatic green-phase crystals. The composition was verified by examination with a Philips 505 SEM and EDAX as corresponding to the stoichiometric green phase.

A crystal with one $(0\bar{1}0)$, four $\{201\}$, two $\{102\}$, two $\{122\}$ and two $\{210\}$ faces and volume $0.115 \times 10^{-3} \text{ mm}^3$ was selected for data measurement. Two independent data sets were measured on a Syntex $P2_1$ diffractometer using graphite-monochromated Mo $K\alpha$ radiation (mean wavelength $\lambda = 0.71069 \text{ \AA}$). As both analyses are consistent within the standard deviations, only those for one data set are recorded here. Unit-cell dimensions were determined from six reflections with $34.79 \leq 2\theta \leq 60.27^\circ$. An analytical absorption correction (Alcock, 1974) and Lorentz and polarization corrections were applied. Variances in measured structure factors $\sigma^2(F_o)$ from counting statistics were modified for source instability using the program *DIFDAT* and increased when necessary by applying the Fisher-test option of program *SORTRF* (Hall & Stewart, 1989) when comparing intensities of equivalent reflections. Full-matrix least-squares-refinement weights $w = 1/\sigma^2(F_o)$ were used for all independent reflections, *i.e.* following good statistical practice, no reflections were classified arbitrarily as 'unobserved'. Experimental and refinement details are listed in Table 1. Atomic form factors and dispersion corrections were taken from *International Tables for X-ray Crystallography* (1974, Vol. IV). The least-squares residual $\sum w|F_o| - |F_c|^2$ was minimized by adjusting one scale, 16 positions and 32 independent vibration parameters, along with \mathbf{r}^*

for the Zachariasen (1969) isotropic secondary-extinction corrections as formulated by Larson (1970). Final shift/e.s.d. < 0.0005 . The computer programs *STARTX*, *DIFDAT*, *ABSORB*, *ADDATM*, *ADDREF*, *FC*, *SFLSX*, *BONDLA*, *FOURR*, *CHARGE*, *CONTRS*, *SLANT* and *PLOT* from the *XTAL2.6* system (Hall & Stewart, 1989), installed on a Sun 280 computer, were used in the analysis. Following Watkins *et al.* (1988) the cell is transformed to the standard *Pnma* setting in this study. Structural parameters are listed in Table 2.*

The atomic positions are close to those reported by Watkins *et al.* (1988) and by Sato & Nakada (1989). The vibration amplitudes do not have the anomalously low values for Y1 and Y2 reported by Watkins *et al.* (1988) and agree more closely with those of Sato & Nakada (1989), although the U_{eq} value of $0.0069 (2) \text{ \AA}^2$ for Ba is lower than the value of $0.00808 (7) \text{ \AA}^2$ reported by those authors. Trends in the vibration amplitudes resemble those for Ba, Cu2 and Y in the high- T_c compound in so far as Ba is relatively labile, Y is tightly bound and Cu shows intermediate behaviour.

Structural geometry

Y_2BaCuO_5 forms an intricate bond network with all cations and the O3 atom coplanar in the (010) plane with $y = 0.25$. As shown in Fig. 1(a), M—O bonds to O1 and O2 link neighbouring planes of cations. There is close correspondence between the sevenfold coordination polyhedra for Y1 and Y2 in this structure. The geometries of the coordination polyhedra for Y1, Y2 and Ba shown in Figs. 1(b), 1(c) and 1(d) differ appreciably from those in the superconducting phase, in which the Y atom is eight-coordinated and the Ba-atom coordination sphere contains O-atom defects. The fivefold coordination of Cu is shown in Fig. 1(e). The Cu atom is displaced from the O1—O2 plane by $0.229 (2) \text{ \AA}$ towards O3 — its structural geometry closely resembling that of Cu2 in $\text{YBa}_2\text{Cu}_3\text{O}_{7-\delta}$.

* Lists of structure factors have been deposited with the British Library Document Supply Centre as Supplementary Publication No. SUP 55495 (10 pp.). Copies may be obtained through The Technical Editor, International Union of Crystallography, 5 Abbey Square, Chester CH1 2HU, England.

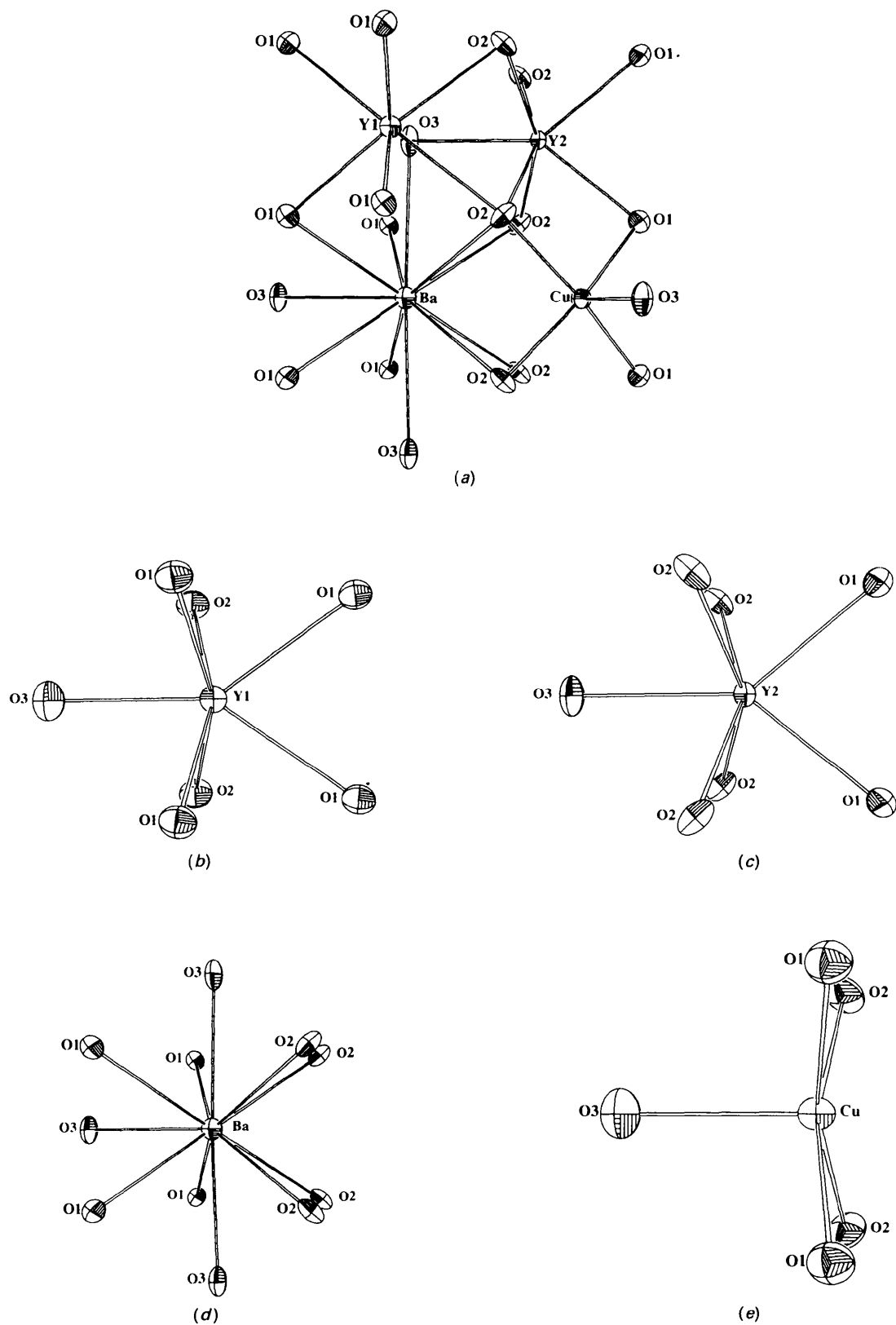


Fig. 1. Y_2BaCuO_5 subunits: (a) structural geometry; (b) Y1 coordination; (c) Y2 coordination; (d) Ba coordination; (e) Cu coordination.

Table 3. Selected interaction-vector lengths (\AA) and $O-M-O'$ angles ($^\circ$) for Y_2BaCuO_5

M is Ba, Y1, Y2 or Cu, with O and O' symmetry-related by reflection across the mirror plane at $y = 0.25$.

Coordination		Interaction			
		length $M-O$	$O-M-O$ angle		
Ba	11	Ba—O3	2.611 (3)	0 (on mirror)	
		Ba—O3	2.832 (1) $\times 2$	O3—Ba—O3	176.22 (9)
		Ba—O2	2.955 (2) $\times 2$	O2—Ba—O2	56.30 (7)
		Ba—O2	3.005 (2) $\times 2$	O2—Ba—O2	57.13 (7)
		Ba—O1	3.066 (2) $\times 2$	O1—Ba—O1	53.34 (7)
Y1	7	Ba—O1	3.250 (2) $\times 2$	O1—Ba—O1	53.17 (7)
		Y1—O3	2.279 (3)	0 (on mirror)	
		Y1—O1	2.297 (2) $\times 2$	O1—Y1—O1	78.56 (9)
		Y1—O1	2.364 (2) $\times 2$	O1—Y1—O1	71.21 (9)
		Y1—O2	2.383 (2) $\times 2$	O2—Y1—O2	74.22 (9)
Y2	7	Y2—O3	2.305 (3)	0 (on mirror)	
		Y2—O1	2.308 (2) $\times 2$	O1—Y2—O1	78.18 (9)
		Y2—O2	2.329 (2) $\times 2$	O2—Y2—O2	73.51 (9)
		Y2—O2	2.352 (2) $\times 2$	O2—Y2—O2	75.33 (9)
		Cu—O1	1.976 (2) $\times 2$	O1—Cu—O1	88.3 (1)
Cu	5	Cu—O2	2.017 (2) $\times 2$	O2—Cu—O2	87.4 (1)
		Cu—O3	2.204 (3)	0 (on mirror)	

 $M-M$ contacts ($< 4.0 \text{ \AA}$)

	Ba	Y1	Y2	Cu
Ba	3.7935 (8) $\times 2$	3.6724 (9) $\times 2$	3.533 (1)	3.2650 (8)
Y1		3.908 (1)	3.6962 (9) $\times 2$	3.5617 (9) $\times 2$
Y2		3.6694 (9) $\times 2$	3.2869 (8)	2.980 (1)
			3.4820 (9)	
			3.6483 (9) $\times 2$	
Y2				2.8234 (9)
				3.148 (1) $\times 2$

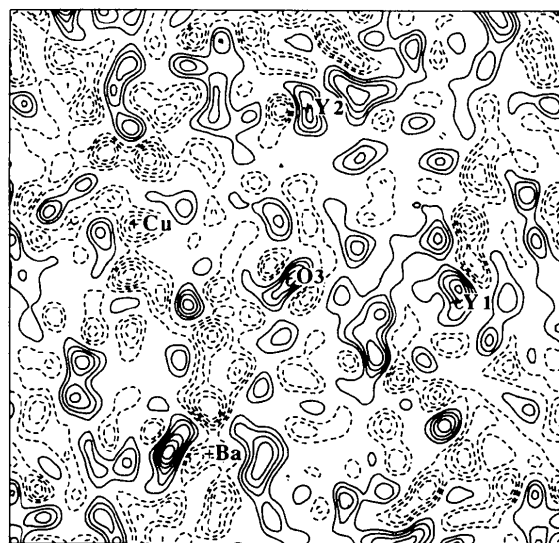
Table 4. Atomic charges based on Hirshfeld partitioning of $\Delta\rho$

Atom	Charge (e)
Ba	-0.2 (2)
Y1	0.7 (1)
Y2	0.6 (1)
Cu	0.3 (1)
O1	-0.34 (8)
O2	-0.33 (8)
O3	-0.04 (8)

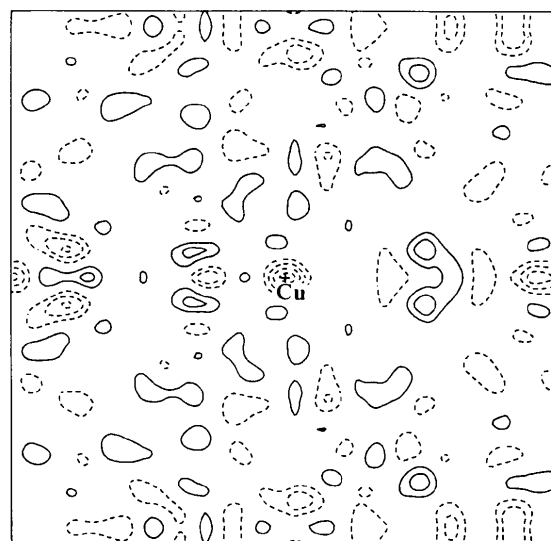
Selected interatomic distances and angles are listed in Table 3. The shortest $M-O$ contacts involving Ba, Y1 and Y2 are with O3 in the $y = 0.25$ plane, whereas Cu—O3 is the longest Cu—O vector. However, that vector is about 0.1 \AA shorter than the value of $2.327 (6) \text{ \AA}$ reported for Cu2—O1 in $YBa_2Cu_3O_{7-\delta}$ (Buttner & Maslen, 1992). The Cu—O1 and Cu—O2 bonds in Y_2BaCuO_5 are correspondingly 0.06 \AA longer than the values of $1.942 (2) \text{ \AA}$ for Cu2—O2 and $1.955 (2) \text{ \AA}$ for Cu2—O3 in the high-temperature superconductor. The Cu geometry for Y_2BaCuO_5 could be regarded as the asymptotic limit that the Cu2 geometry in $YBa_2Cu_3O_{7-\delta}$ approaches as δ for that structure decreases. It is difficult to sustain the argument that the valence state for Cu2 in that structure changes with O-atom content based on coordination geometry alone.

Atomic charges

Atomic charges, determined by projecting the difference density $\Delta\rho$ onto atomic density basis functions following the method of Hirshfeld (1977), are listed in Table 4. The large standard deviations in these charges reflect the limitations on accuracy imposed by the high atomic numbers of the cations in this structure. Nevertheless, there is close agreement between the Y1 and Y2 values, which have similar coordination, and likewise between those for O1 and O2. The broad trends among the charges reflect atomic electronegativities, modulated



(a)



(b)

Fig. 2. $\Delta\rho$ for Y_2BaCuO_5 , contour intervals $1.0 e \text{ \AA}^{-3}$, positive contours solid, negative contours broken. (a) $y = 0.25$, map size $7.6 \times 7.2 \text{ \AA}$; (b) section through Cu parallel to the plane O1—O2—O2—O1, map size $6.2 \times 6.0 \text{ \AA}$.

by packing density in the manner noted for comparable structures such as KCuF₃ (Buttner, Maslen & Spadaccini, 1990). That is, for two atoms with the same atomic number, electrons accumulate preferentially on the one that is less tightly packed. Thus O1 and O2, with few short *M*—O bonds, carry larger negative charges than O3, which is centred on the tightly packed $y = 0.25$ plane. Likewise, the positive charges for Y1 and Y2, indicated by their vibration amplitudes to be tightly packed, are larger than those on Cu and *a fortiori* on Ba.

Difference density

The consistency of the charges determined by integrating $\Delta\rho$ indicate that it contains chemically significant information. This is supported by the comparable heights of the density at the atomic positions for Y1 and Y2 shown for the plane $y = 0.25$ in Fig. 2(a). The extrema values of $\Delta\rho_{\min}$ and $\Delta\rho_{\max}$ are within 0.6 Å of the Ba nucleus as reported by Sato & Nakada (1989). In so far as the topography of the $\Delta\rho$ map does not correlate closely with the nearest neighbour O-atom geometry around Ba and Y, it resembles that in YBa₂Cu₃O_{7- δ} . There is an approximate centre of symmetry in the $\Delta\rho$ map within 1 Å of the Ba nucleus. This is to be expected if *s* and *d* states predominate in the Ba-bonding interactions. The electron density near Ba is depleted most strongly in the solid angle subtended by the adjacent CuO₅ moiety, whereas electrons accumulate outside those angles. The topology of the $\Delta\rho$ map in Fig. 2(a) is complex and its relationship to the interactions is not obvious. A detailed examination showed that the features near the Y1, Y2 and Ba atoms satisfy the following principles. The electron density within any small O—*M*—O angles between short *M*—O vectors is depleted. That electron density is transferred to the larger O—*M*—O angles with long *M*—O vectors. These characteristics indicate exchange to be the main factor determining the topology of the difference density. Near Cu $\Delta\rho$ has the approximate centre shown in Fig. 2(b).

The depletion of density near Cu also has no obvious relationship to the O-atom coordination, which would be a discouraging result except that it is also true of the corresponding density around Cu2 in YBa₂Cu₃O_{7- δ} . That is, the density does not have the strongly developed lobes of negative $\Delta\rho$ observed in most Jahn–Teller-distorted copper(II) systems and near Cu1 in YBa₂Cu₃O_{7- δ} . There is no evidence in the $\Delta\rho$ topography that the electronic state for Cu in Y₂BaCuO₅ differs from that of Cu2 in YBa₂Cu₃O_{7- δ} . Because both the structural geometry and the difference densities near Cu and Cu2 are comparable it is likely that the electronic state for these atoms in the two structures is essentially the same.

The contributions of computer programs by their authors – R. Alden, G. Davenport, R. Doherty, W. Dreissig, H. D. Flack, S. R. Hall, J. R. Holden, A. Imerito, R. Merom, R. Olthof-Hazenkamp, M. A. Spackman, N. Spadaccini and J. M. Stewart – to the XTAL2.6 system (Hall & Stewart, 1989), used extensively in this work, is gratefully acknowledged. This research was supported by the Australian Research Council.

References

- ALCOCK, N. W. (1974). *Acta Cryst.* **7**, 838–842.
 BUTTNER, R. H. & MASLEN, E. N. (1992). *Acta Cryst.* **B48**, 21–30.
 BUTTNER, R. H., MASLEN, E. N. & SPADACCINI, N. (1990). *Acta Cryst.* **B46**, 131–138.
 HALL, S. R. & STEWART, J. M. (1989). Editors. *XTAL2.6 Users Manual*. Univs. of Western Australia, Australia, and Maryland, USA.
 HIRSHFELD, F. H. (1977). *Isr. J. Chem.* **16**, 198–201.
 LARSON, A. C. (1970). *Crystallographic Computing*, edited by F. R. AHMED, pp. 291–294. Copenhagen: Munksgaard.
 MICHEL, C. & RAVEAU, B. (1982). *J. Solid State Chem.* **43**, 73–80.
 SATO, S. & NAKADA, I. (1989). *Acta Cryst.* **C45**, 523–525.
 WATKINS, S. F., FRONCZEK, F. R., WHEELLOCK, K. S., GOODRICH, R. G., HAMILTON, W. O. & JOHNSON, W. W. (1988). *Acta Cryst.* **C44**, 3–6.
 ZACHARIASEN, W. H. (1969). *Acta Cryst.* **A25**, 102.